Transparent fire protective sol-gel coating for wood panels

Séverine Bellayer, Alexandre Gossiaux, Sophie Duquesne, Benjamin Dewailly, Pierre Bachelet, Maude Jimenez

Polymer Testing 110 (2022) 107579

Contents lists available at ScienceDirect

Polymer Testing

journal homepage: www.elsevier.com/locate/polytest

Transparent fire protective sol-gel coating for wood panels

Séverine Bellayer *, Alexandre Gossiaux, Sophie Duquesne, Benjamin Dewailly, Pierre Bachelet, Maude Jimenez

Univ. Lille, CNRS, INRAE, Centrale Lille, UMR 8207, UMET, Unité Matériaux et Transformations, F59000, Lille, France

A B S T R A C T

A transparent fire protective sol-gel coating deposited on wood has been evaluated using different fire tests, such as mass loss cone, mini single burning item and furnace tests. The heat release rate and total heat release during combustion, but also the flame spread behavior and the thermal protection performances of the coatings have been studied. Two processes to apply the sol-gel coating on wood have been assessed to show the thickness dependence of the fire performance. When deposited as a thick coating (800 μm thick) on wood, the sol-gel coating lowers the total heat release, decreases the flame spread and greatly improves the thermal protection of the substrate.

1. Introduction

In recent years, transparent flame retardant coatings have attracted a lot of attention, especially in the field of wood, where it is important to keep the natural appearance. In the literature, several studies report the design of transparent fire-protective coatings for wood. For instance, Xu et al. [1,2], as well as Yan et al. [3–5] reported the modification of amino matrices with various flame retardant additives such as phosphate modified sepiolite, layer double hydroxide, graphite oxide, zinc borate or boron-containing flame retardants. Shi et al. focused on the introduction of functional groups and flame retardant groups such as polyethylene glycol [6], epoxy resin [7], and silicon-containing epoxy compounds [8] into the structure of phosphorus-containing compounds based on 1-oxo-4-hydroxymethyl-2,6,7-trioxa-l-phosphabicyclo[2.2.2] octane (PEPA), and then applied them as flame retardants in amino transparent intumescent fire-retardant coatings. Based on their work, the best flame-retardant properties were obtained using silicon-containing epoxy/PEPA phosphate transparent intumescent fire resistant coating. The synergistic effect between phosphorous and silicon improved the foam structure and enhanced the fire protection properties of the coatings (intumescence during burning, more thermally stable).

Chen et al. [9] propose to directly modify cellulose with 9,10-dihydro-9-oxa-10-phosphaphenanthrene-10-oxide (DOPO) to promote the production of a dense and continuous char during combustion. Carosio et al. [10] used transparent cellulose nanofiber (CNF) and clay nanocomposites to build a FR brick-and-mortar structure at the wood surface. In the same way, Liu et al. [11] synthesized transparent flame-retardant ceramic coatings via the sol-gel method using siloxane and silica sol with organophosphates.

A sol-gel-derived hybrid coating solution improves the flame-retardant properties of treated substrates by acting as a thermal insulator. A silica sol-gel architecture is an inorganic structure, which is by itself unable to act in the gas phase; it operates only in the condensed phase during the combustion of a polymeric material. To overcome this limitation, our lab managed to formulate hybrid silica sol-gel by combining the silica phase with active species (phosphorus and nitrogen), leading to synergistic or joint effects acting in both condensed and gas phases. This coating was developed for flexible polyurethane (PU) foam; it is made of a mixture of tetraethoxysilane (TEOS), methyl triethoxysilane (MTES), 3-aminopropyl triethoxysilane (APTES) and diethyl phosphite (DEP) in an ethanol/water solution with Tin II 2 ethylhexanoate (TEH) used as the catalyst. The coating shows an intumescent behavior upon burning exhibiting significant expansion and bubbling [12,13]. The coating allows the protection of the underlying PU foam during burning as well as the reduction of the amount of smoke released.

Intumescent flame-retardant systems are usually composed of three active ingredients: an acid source, a carbon source, and a blowing agent [14]. When heated, they can swell and form a thick porous layer, which acts as a thermal barrier to protect the substrate from flame or heat. Most of these fire protective coatings are opaque, due to either the poor compatibility of the fire-retardant additives with the matrix resin or the filler sizes. Since the sol-gel coating developed in our lab is transparent, it was thus considered as potentially interesting for wood.

Two different processes of deposition were studied, one by impregnation and the other by gel coating in order to create different coating

* Corresponding author.
E-mail address: severine.bellayer@univ-lille.fr (S. Bellayer).

https://doi.org/10.1016/j.polymertesting.2022.107579
Received 7 February 2022; Received in revised form 31 March 2022; Accepted 4 April 2022
Available online 11 April 2022

thicknesses and evaluate their fire behavior when deposited on top of wood panels. Cone calorimeter experiments were performed on the wood plates treated with thin or thick sol-gel coatings to evaluate their reaction to fire and the flame spread during burning was monitored using a small-scale single burning item (SBI) test developed in our lab. In order to better understand the mechanism of action of the sol-gel coating, the fire resistant property of the coating alone was also tested using a small-scale furnace test following the ISO-834 normalized temperature/time curve.

2. Experimental part

2.1. Raw materials

Chemical products, i.e., tetraethoxysilicate (TEOS, 98% purity), methyltriethoxysilicate (MTES, 95% purity),3-aminopropyl triethoxysilane (APTES, 97% purity), diethyl phosphite (DEP, 99% purity), tin II 2 ethylhexanoate (TEH, 92.5–100% purity) and titanium diisopropoxide bis(acetylacetonate) (TDBA, 75 wt% in isopropanol) were purchased from Sigma Aldrich, France and used as received. Hydrochloric acid (HCl, 37% purity) was purchased from VWR Internationals, France. Resorcinol bis(diphenyl phosphate) (Fyrolflex RDP) was purchased from ICL. Wood substrates used for mass loss cone were 2.2 cm × 10 cm x 10 cm pine samples cut from raw pine cleats (80 g+/-2%). Wood panels used with the small scale SBI were 50 cm × 33 cm and 50 cm × 16 cm laminated pine samples. To investigate the thermal resistance properties of the coating, 3 mm*100 mm*100 mm, classical XC38 steel plates were used, provided by Tartaix, France.

2.2. Sol-gel process

Sol-gel process starts as a liquid, which reticulates and becomes a gel and then a solid over time. The sol-gel solutions optimized in our lab for PU foams [12,13] were prepared using 10.8 ml of EtOH, 5.8 ml of TEOS, 1.44 ml of MTES, 12 ml of APTES, and 6.5 ml of DEP. These chemicals were added in that order before adding 216 ml of distilled water. 0.3 ml TEH catalyst was then added drop by drop to the solution. It was optimized to create thin coatings by impregnation.

To produce thick coatings, the sol-gel solution was left to dry for two days in aluminum foil, to obtain a gel, viscous enough to be applied with a spatula on top of the wood.

2.3. Optical microscopy

Prior to the observation, the samples were cut, embedded into epoxy resin and polished. An ESCIL manual polisher was used to polish the samples, using SiC polishing sheets from grade 80 up to grade 4000. To observe the coating cross section of the samples, a Keyence VHX 1000 optical microscope was used, with a Z20 objective (from X20 up to X200 magnification).

3. Fire tests

3.1. Mass loss cone

A Fire Testing Technology (FTT) Mass Loss Calorimeter (MLC) was used to perform measurements on samples following the procedure ASTM E 906 [15]. The equipment is identical to that used in oxygen consumption cone calorimetry (ISO 5660), except that a thermopile in the chimney is used to obtain the heat release rate (HRR) rather than employing the oxygen consumption principle. Wood samples (10 cm × 10 cm × 2.2 cm) were tested in horizontal orientation. Samples were then wrapped in aluminum foil, leaving the upper surface exposed to the heater (external heat flux = 50 kW/m^2) and placed on a ceramic backing board at a distance of 35 mm from cone base. MLC was used to determine the following fire properties: heat release rate (HRR) as a function of time, peak of heat release rate (pHRR) and total heat release (THR). All values were calculated using FTT's MLC calculation software. Tests were performed three times to ensure reproducibility.

3.2. Single burning item (SBI)

The small scale SBI (Fig. 1) is a test developed in our lab at the University of Lille, France [16]. The main idea is to reduce the scale of the real SBI test (ISO 13823 standard) [17] to 1/3 in order to make it more versatile and less costly. The data acquisition process is identical to the real test, that is to say, 5 min burner calibration before the 21 min panel combustion. The size of the sample is reduced by 1/3, however, its thickness has to be taken into account and added to the width of the panel due to the overlapping of the panels in the corner. Contrary to the sample size, the burner heat flow is not reduced by 1/3. Indeed, with a heat flow of 10 kW the flame completely covers the sample. For this purpose, the propane flow rate has been adjusted to 0.08 kg/h. To better monitor the flame spread during combustion, an IR camera was set up to measure the surface temperature during whole combustion. A FLIR X6540sc IR camera calibrated from 20 °C to 1500 °C was used, equipped with a specific filter-eliminating wavelength corresponding to the flame. It allows the visualization of the surface of a material without the contribution of the flame. The data was collected and treated with FLIR ResearchIR software.

3.3. Small-scale furnace test

To evaluate the fire performance of intumescent coatings in a fire scenario, a small-scale furnace test was developed. The furnace window (vertical flat panel) is designed for 10 × 10cm [2] samples (Fig. 2). This test was designed to be able to mimic the ISO-834 [18] normalized temperature/time curve. Refractory fibers stable up to 1300 °C cover the inside of the furnace. The furnace is equipped with two burners fed with propane gas having a capacity of 20 kW each. The propane flow is regulated to mimic an ISO-834 curve. A thermocouple connected to a regulator is placed in the oven to control the flow rate of propane gas in the oven in real-time during the experiment. Thus, the real-time temperature in the oven is known at all times and corrected to follow the set point temperature. Small furnace fire tests was performed according to the standard curve of ISO-834 (cellulosic fire test, Fig. 3). This normalized time-temperature curve follows the equation:

$$T = 345\log_{10}(8t + 1) + 20$$

where t is the time in minutes (min) and T the average temperature of the oven in degrees Celsius (°C).

In the conditions of the furnace test, the backside of each sample was painted in black with a Jelt heat resistant black matte paint to keep a constant emissivity and the temperature was read with a Raytek PhotoTemp MX pyrometer while the temperature rose in the furnace.

4. Results and discussions

The first step of the study was to choose the operating mode of deposition of the sol-gel at the surface of the wood. Thus, two different deposition processes were assessed. For the first deposition process the wood substrate was immersed in the sol-gel solution and left for 12 h at 60 °C in an oven, for optimizing impregnation. The second process consisted in letting the sol-gel solution turn into a gel at 60 °C in an oven for 48 h. When the gel was viscous enough, it was deposited on the wood surface with a spatula. In both cases, after deposition, the sample was left to dry for at least 48 h at 60 °C in an oven to remove all traces of solvent and water. Results can be observed in Fig. 4. The images show the aspect of each sample before mass loss cone experiments. After the immersion process the coating is very thin and the wood becomes yellowish, but after gel coating with the spatula, the wood becomes

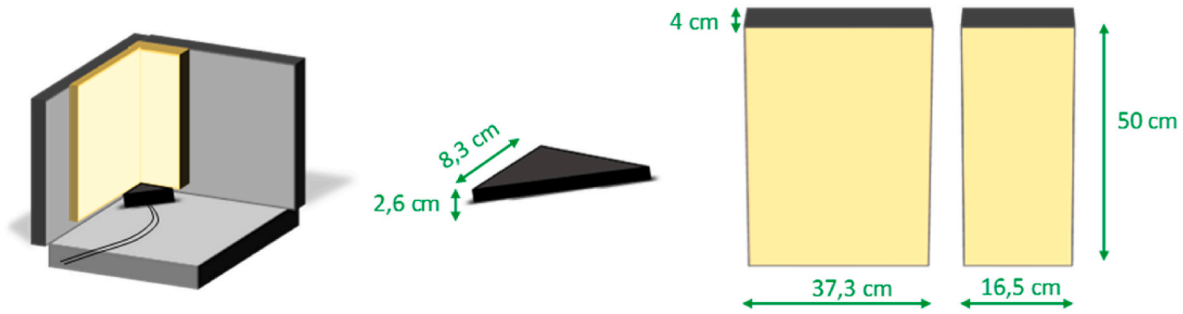

Fig. 1. Schema and dimension of the small scale SBI.

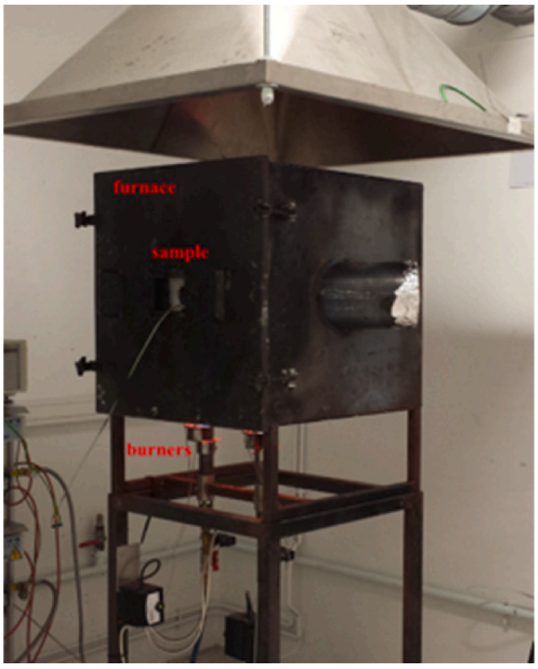

Fig. 2. Image of the small furnace fire test 10 cm*10 cm.

shiny; the coating is thick, transparent, homogenous and smooth.

The two coated samples were cut, impregnated into epoxy resin and polished to measure the thickness of the coating in each case (Fig. 5). When the wood is immersed in the sol-gel, the obtained coating is thin, 80 μm (2.6 g, 2,5% weight gain), compared to the coating applied with a spatula. In that case, any kind of coating thickness can be obtained. Here, it was decided to coat the wood with a thick coating of 800 μm (6.3 g, 7,9% weight gain). The wood samples with or without coating were left to dry in an oven at 50 °C for at least 48 h h prior to MLC tests.

Fig. 6 shows the HRR curves versus time for the three samples: virgin, FR-impregnated and FR-gel coated wood. Table 1 shows the different characteristic values of the MLC results for the three samples. It can be seen that when the wood is only immersed in the sol-gel solution before gelation, the HRR curve is similar to the one of the virgin wood. The values of pHRR and of THR are also similar; THR for the immerged wood is 56 MJ/m^2 compared to 60 MJ/m^2 for the virgin wood, and pHRR is 115 W/m^2 for the FR-impregnated wood compared to 110 W/m^2 for the virgin wood. When the wood is coated with the gel, the THR significantly decreases by 25% down to 44 MJ/m^2; however, the pHRR remains unchanged around 110 W/m^2. It can be seen that the gel coating process decreases the THR, but it increases the flaming time from 1700 s up to 3000 s. Thus, after a similar quick and intense pHRR at ignition time, the combustion is less intense but longer lasting than that of the virgin wood. In terms of time to ignition, it can be seen that the sol-gel treatment, whatever the process, decreases the time to ignition.

It was noticed with the MLC curves that results obtained for the virgin and FR-impregnated wood were quite similar. Fig. 7 shows the chars of the different samples obtained after MLC tests. It is noticeable that when the sample is impregnated with the sol-gel solution, the top of the char remains compact; however, many cracks appear, which contribute to heat propagation through the sample and to sustaining the combustion. The thin coating obtained using this immersion process is not strong enough: it cracks during combustion and does not protect the underlying layers from the 50 kW/m^2 heat flux. When the wood is coated with the thick gel, the coating is stronger and protects the wood

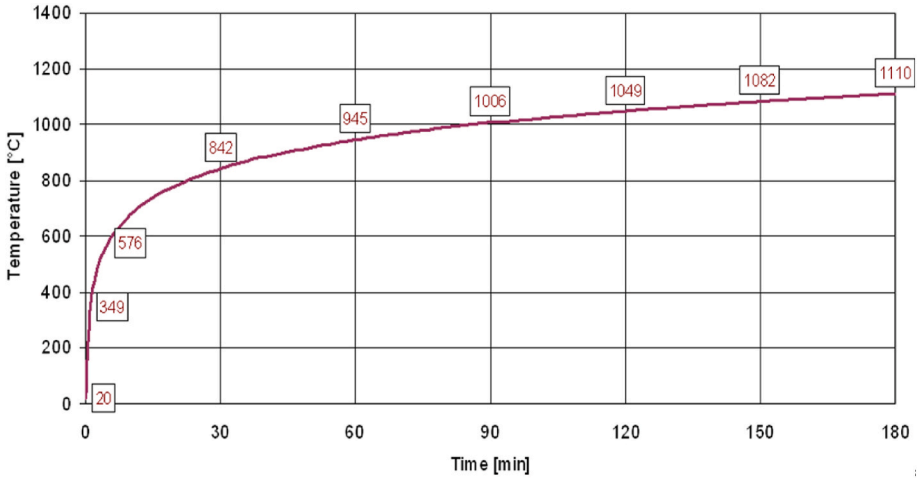

Fig. 3. Standard curve of ISO-834.

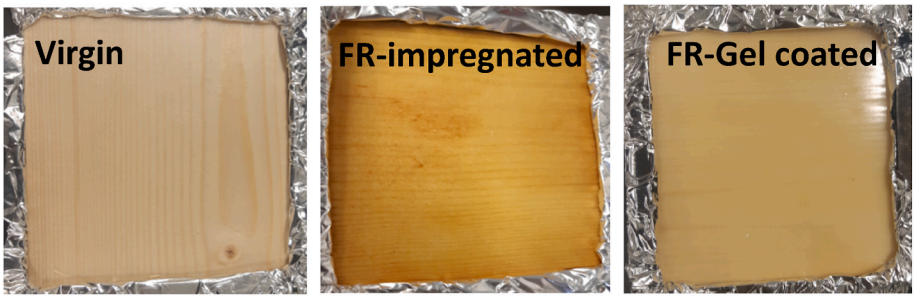

Fig. 4. Images of the wood without coating (virgin), after immersion in sol-gel solution (FR-impregnated) and after sol-gel coating with a spatula (FR-gel coated).

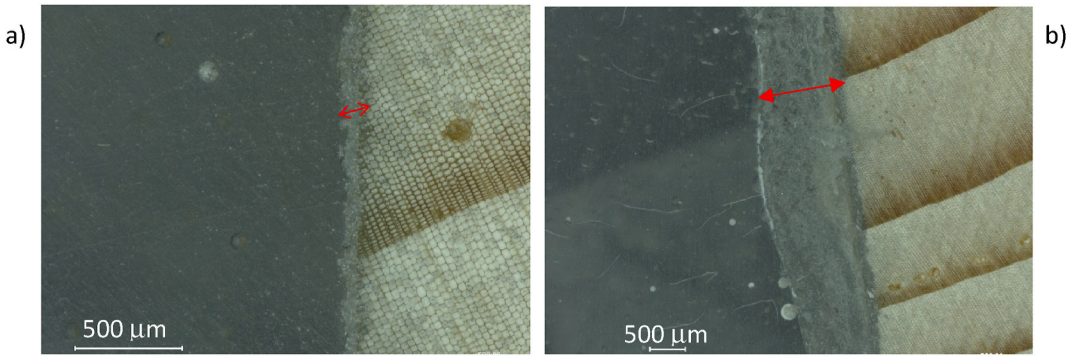

Fig. 5. Images of the coating cross sections (red arrows) of the wood after immersion in sol-gel solution (a, x150) and after gel coating with a spatula (b, x50).

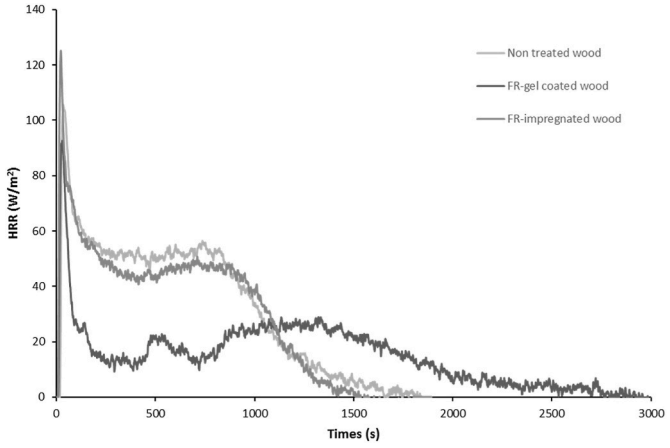

Fig. 6. HRR curves of the virgin, the FR-impregnated and the FR-gel coated wood samples.

Table 1
MLC values for the virgin wood, the FR-impregnated wood and the FR-gel coated wood.

Samples	pHRR (W/m^2)	THR (MJ/M^2)	Flaming time (s)	Time to ignition (s)
Virgin wood	110	60	1700	20
FR-Impregnated wood	115	56	1500	7
FR- gel coated wood	105	44	3000	10

for a longer time. The char shows only one big crack. Our hypothesis is that the second peak observed for the FR-gel coated sample (between 800s and 2000s) appears when the surface of the sample starts to crack.

The MLC test thus shows that the gel deposition process slows the combustion of the wood. Under the MLC test conditions, the whole sample is under the heat source, and no flame spread can be measured. Thus, in order to verify that the coating does not promote flame spread, large samples of wood were coated with the FR-gel coating process and tested with a mini SBI test. Since the FR-impregnated sample did not demonstrate any FR improvement under the MLC test, only the FR-gel coated sample was tested. During the test, the surface temperature was recorded with an IR camera to follow the temperature increase and monitor the flame spread throughout the whole test. To compare the virgin and FR-gel coated samples, the data were treated with the IR camera software. Fig. 8a and b show the images taken with the IR camera after 900s for the virgin and FR-gel coated woods exposed to the mini SBI test. The surface temperatures are color coded; red color relates to high temperatures whereas blue corresponds to low temperatures. Visually, the burning area of the wood seems smaller for the treated sample than for the non-treated one. To better compare both results, temperature values were recorded, and temperature profiles were built (Fig. 8c). Fig. 8c shows the two temperature profiles of the virgin FR-gel coated wood. The temperature profiles allow us to see the flame spread along the wood panel, since the temperature increases where the flames are located. It is noticeable that the width of the peak of temperature is more significant for the non-coated wood than for the FR-gel coated wood. Thus, the flame has a slight tendency to spread when the wood is not coated, which is not the case when the coating is applied to the surface of the wood.

Fig. 9 shows one side of the samples after the SBI test. The pictures were taken from the front (a and b) and the cross section (c and d). The cross section pictures were taken after having cut the sample with a circular saw along the dotted line in the images. The length of the degraded area (black area) is smaller for the coated wood. The coating prevented the flame from spreading at the surface of the wood. The more significant difference comes from the cross section images, where it can be noticed that the wood is almost not burned below the coating (only one or 2 mm) compared to the virgin wood, which is deeply degraded (over 1 cm). The treated wood has been protected by an intumescent char (8 mm thick), visible in the image, above the wood.

Fig. 7. Digital pictures of the chars of the virgin, FR-impregnated and FR-gel coated wood samples.

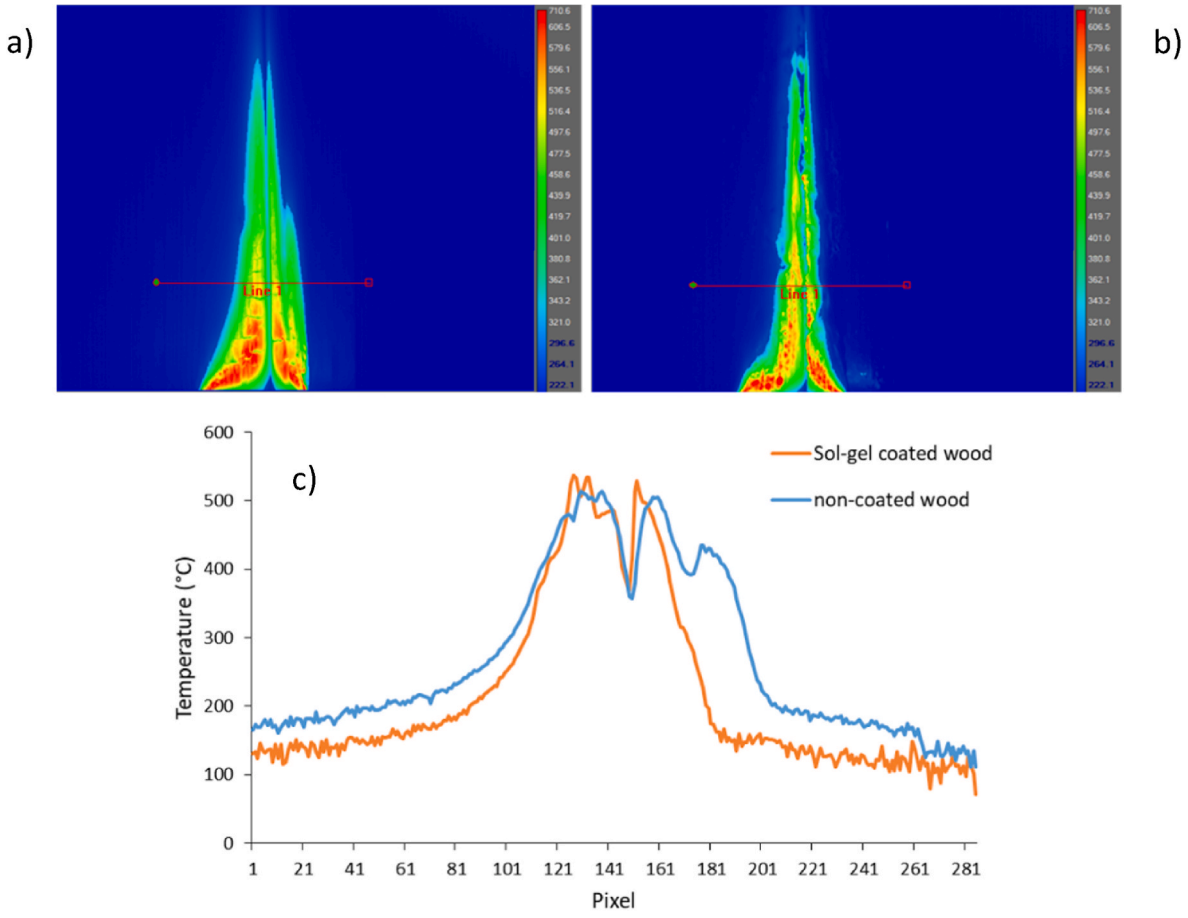

Fig. 8. Infrared images of the virgin wood a) and FR-gel coated wood b), and the corresponding temperature profiles c) along the red line for each two samples. (For interpretation of the references to color in this figure legend, the reader is referred to the Web version of this article.)

Thus, the FR-gel coating seems to be a good thermal insulator and protects the wood from further degradation. To verify this assumption, a comparison of thermal protection was made between a virgin metal plate and a metal plate coated with 800 μm FR-gel in furnace test conditions. Fig. 10 shows the temperature versus time curves for the two samples. The backside of the virgin metal plate reaches 500 °C quickly (700 s), whereas when the metal plate is gel coated, the temperature rise is slowed and more time is required to reach 500 °C (1800 s). The coating thus appears to be a good thermal barrier. At around 120 °C, a change in the curve slope is noticeable (red arrow) for the FR-gel coated metal plate. This temperature corresponds to the beginning of the swelling of the coating, well characterized in a previous paper [13]. The expansion occurs in two steps: a first step around 190 °C, related to the release of ethanol, and a second one around 380 °C, related to the release of non-degraded DEP, ammonia and propylene during degradation of the PU matrix. The flame retardant effect occurs (i) in the condensed phase by intumescence, which yields a thermal insulating layer made of a SiO2 and Si–O–P network mixed with orthophosphate at the surface of the PU foam, but also (ii) in the gas phase by the release of non-degraded DEP, which acts as free radical scavenger. This coating creates a 3D silicon network upon burning, which slows down the release of degradation products and protects the underlying flexible polyurethane foams from burning.

The residue of the coating after the furnace test is still adherent to the plate, and the swelling can be observed after the test in Fig. 11. The maximum of the swelling does not occur in the middle of the plate but at the bottom of the plate. The metal plate being placed vertically in the furnace implies that the coating flows down slightly during the test,

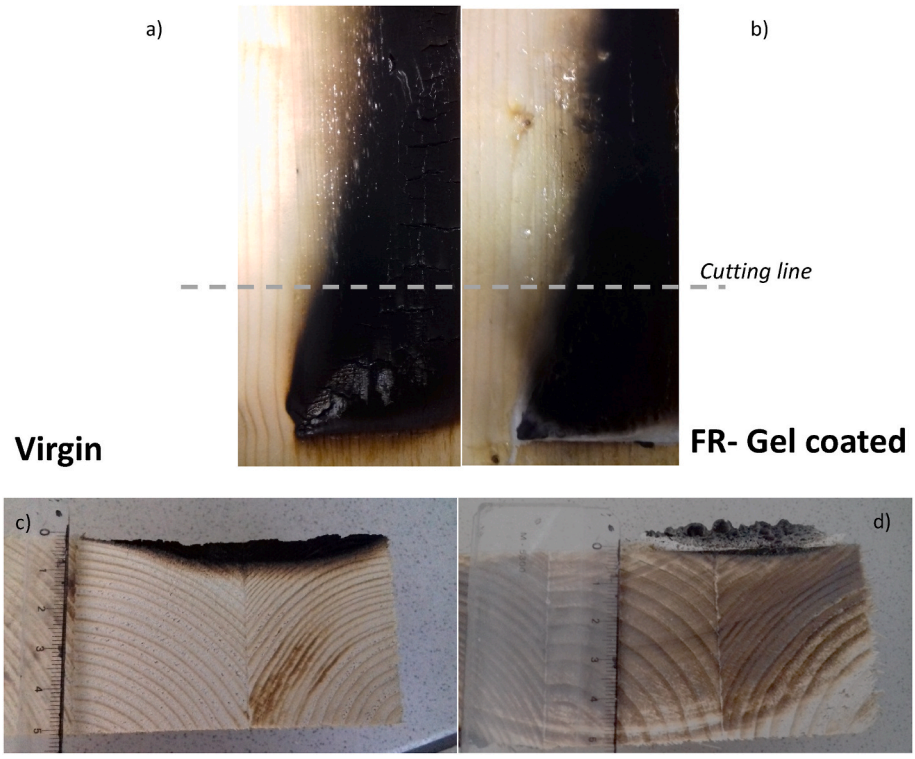

Fig. 9. Images of one corner side of the small-scale SBI residues of the virgin and FR-gel coated wood samples (a and b respectively) from the front and of the virgin and FR-gel coated wood samples (c and d respectively) from the side.

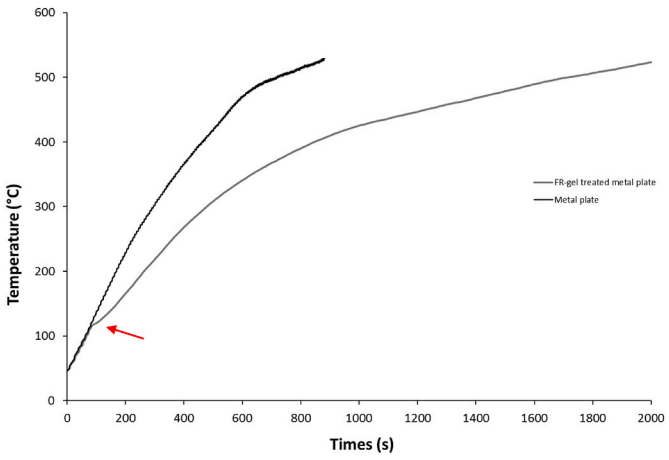

Fig. 10. Temperature versus time curves comparing the virgin metal and FR-gel coated metal plates.

probably due to a viscosity decrease during temperature rise. Thus, despite the flowing behavior during temperature rise, the coating appears to be a good thermal protective barrier that can efficiently protect both wood and steel.

5. Conclusion

In the present study, a transparent sol-gel coating has been tested to flame retard wood panels. First, two different processes were assessed to deposit the sol-gel coating at the surface of the wood plate: an impregnation process and a gel deposition process. The impregnation process leads to a thin coating (80 μm), whereas the gel deposition process leads to a thick coating (800 μm). Under mass loss cone conditions, the thin coating does not lead to any improvement of the FR properties; however, the gel coating process (thick coating) slightly improves the FR properties by decreasing the pHRR and the THR. Further FR characterizations of the gel coating were carried out. When applied on wood panels and submitted to small-scale SBI conditions, the thick coating reduced the flame spread at the surface of the coated wood panels, as well as the degradation process through the wood. The gel coating thermal properties were evaluated using a furnace test and results show that the thick

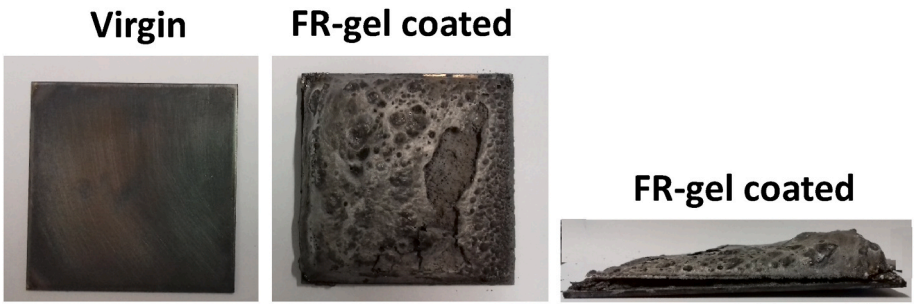

Fig. 11. Images of the samples after the furnace test: the metal plate and the FR-gel coated metal plate from the front and the side.

gel coating has the ability to thermally protect the underlying layers of a sample when exposed to a flame.

Data availability

The raw/processed data required to reproduce these findings cannot be shared at this time as the data also forms part of an ongoing study.

Author statement

Description of the authors' diverse contributions to the published work:

Séverine Bellayer: Conceptualization, Methodology, Writing-Original draft preparation. **Alexandre Gossiaux**: Investigation, Resources. **Sophie Duquesne**: Resources, Supervision. Benjamin Dewailly: Investigation, Resources. **Pierre Bachelet**: Investigation, Resources. **Maude Jimenez**: Supervision, Reviewing.

Declaration of competing interest

The authors declare that they have no known competing financial interests or personal relationships that could have appeared to influence the work reported in this paper.

References

[1] Z. Xu, D. Liu, L. Yan, Xie, Synergistic effect of sepiolite and polyphosphate ester on the fire protection and smoke suppression properties of an amino transparent fire-retardant coating X, Prog. Org. Coating 141 (2020) 105572.
[2] Z. Xu, N. Deng, L. Yan, Flame retardancy and smoke suppression properties of transparent intumescent fire-retardant coatings reinforced with layered double hydroxides, J. Coating Technol. Res. 17 (1) (2020) 157–169.
[3] L. Yan, Z. Xu, N. Deng, Synthesis of organophosphate-functionalized graphene oxide for enhancing the flame retardancy and smoke suppression properties of transparent fire-retardant coatings, Polym. Degrad. Stabil. 172 (2020) 109064.
[4] L. Yan, Z. Xu, X. Wang, Synergistic flame-retardant and smoke suppression effects of zinc borate in transparent intumescent fire-retardant coatings applied on wood substrates, J. Therm. Anal. Calorim. 136 (4) (2019) 1563–1574.
[5] L. Yan, Z. Xu, N. Deng, Effects of Polyethylene Glycol Borate on the Flame Retardancy and Smoke Suppression Properties of Transparent Fire-Retardant Coatings Applied on Wood Substrates Progress in Organic Coatings, vol. 135, 2019, pp. 123–134.
[6] Y. Shi, G. Wang, An intumescent flame retardant containing caged bicyclic phosphate and oligomer: synthesis, thermal properties and application in intumescent fire resistant coating, Prog. Org. Coating 90 (2016) 83–90.
[7] Y. Shi, G. Wang, The novel epoxy/PEPA phosphate flame retardants: synthesis, characterization and application in transparent intumescent fire-resistant coatings, Prog. Org. Coating 97 (2016) 1–9.
[8] Y. Shi, G. Wang, The novel silicon-containing epoxy/PEPA phosphate flame retardant for transparent intumescent fire resistant coating, Appl. Surf. Sci. 385 (2016) 453–463.
[9] Z. Chen, P. Xiao, J. Zhang, W. Tian, R. Jia, H. Nawaz, K. Jin, J. Zhang, A facile strategy to fabricate cellulose-based, flame-retardant, transparent and anti-dripping protective coatings, Chem. Eng. J. 379 (2020) 122270.
[10] F. Carosio, F. Cuttica, L. Medina, L.A. Berglund, Clay Nanopaper as Multifunctional Brick and Mortar Fire Protection Coating-Wood Case Study Materials and Design, vol. 93, 2016, pp. 357–363.
[11] J. Liu, C. Wang, Z. Jiang, Q. Wang, L. Li, Preparation and Characterization of Water-Base Transparent Flame-Retardant Ceramic Coatings for Wood via Sol-Gel Method Advanced Materials Research 482-484, 2012, pp. 1085–1088.
[12] S. Bellayer, M. Jimenez, S. Barrau, S. Bourbigot, Fire retardant sol-gel coatings for flexible polyurethane foams, RSC Adv. 6 (2016) 28543–28554.
[13] S. Bellayer, M. Jimenez, B. Prieur, B. Dewailly, A. Ramgobin, J. Sarazin, B. Revel, G. Tricot, S. Bourbigot, Fire retardant sol-gel coated polyurethane foam: mechanism of action, Polym. Degrad. Stabil. 147 (2018) 159–167.
[14] S. Duquesne, S. Magnet, C. Jama, R. Delobel, Intumescent paints: fire protective coatings for metallic substrates, Surf. Coating. Technol. 180–181 (2004), 302-3072004.
[15] ASTM E906/E906M-17, Standard Test Method for Heat and Visible Smoke Release Rates for Materials and Products Using a Thermopile Method, ASTM International, West Conshohocken, PA, 2017.
[16] A. Gossiaux, P. Bachelet, S. Bellayer, S. Orties, A. König, S. Duquesne, Small-scale single burning item test for the study of the fire behavior of building materials, Fire Saf. J. (2021) 103429.
[17] ISO 13823:2008 (E), General Principles on the Design of Structures for Durability, 2008.
[18] ISO-834, Fire Resistance Tests — Elements of Building Construction, 1999.